RESPIRATORY CARE Paper in Press. Published on July 02, 2013 as DOI: 10.4187/respcare.02568

Revised Article

Growth of Nasal-Laryngeal Airways in Children and Their Implications in Breathing and Inhaled Aerosol Dynamics

[1,*]Jinxiang Xi PhD, [2]Xiuhua Si PhD, [3]Yue Zhou PhD, [1]JongWon Kim PhD, and [4]Ariel Berlinski MD

[1]Department of Mechanical and Biomedical Engineering, Central Michigan University, Mount Pleasant, MI

[2]Department of Engineering, Calvin College, Grand Rapids, MI

[3]Aerosol and Respiratory Dosimetry Program Lovelace Respiratory Research Institute, Albuquerque, NM

[4]Department of Pediatrics, University of Arkansas for Medical Science, Little Rock, AR

Running title: *Nasal Airway Growth and Implications in Children*

Dr Jinxiang Xi presented a version of this paper at the 58th AARC Congress, held November 10-13, 2012, in New Orleans, Louisiana, at which, for the paper he was awarded the Monaghan-Trudell Fellowship for Aerosol Technique Development from the American Respiratory Care Foundation.

The study performed collaboratively in Central Michigan University, Mount Pleasant MI and Lovelace Respiratory Research Institute, Albuquerque, NM.

The use of these images has been approved by the UAMS Institutional Review Board.

The authors have declared no conflicts of interest.

*Corresponding author: Jinxiang Xi PhD
Address: Department of Mechanical and Biomedical Engineering
Central Michigan University
1200 South Franklin Street
Mount Pleasant, MI 48858
Phone: (989) 774-2456
Fax: (989) 774-4900
Email: xi1j@cmich.edu

RESPIRATORY CARE Paper in Press. Published on July 02, 2013 as DOI: 10.4187/respcare.02568

BACKGROUND: The human respiratory airway undergoes dramatic growth during infancy and childhood, which induces significant variability in airflow pattern and particle depositions. However, deposition studies have typically focused on adult subjects, results of which may not be readily extrapolated to children.

OBJECTIVE: To quantify the growth of human nasal-laryngeal airways at early ages, and to evaluate its impact on breathing resistance and respirable aerosol deposition.

METHODS: Four image-based nasal-laryngeal models were developed from children of different ages (10-day to 5-year old) and were compared to that of an adult. The airway dimensions were quantified in terms of different parameters (volume, cross-section area, and hydraulic diameter) and of different anatomies (nose, pharynx, and larynx). Breathing resistance and aerosol deposition were computed using a high-fidelity fluid-particle transport model and validated against *in vitro* measurements in replica casts fabricated from the same airway models.

RESULTS: Significant differences in nasal anatomy were observed among the five subjects in both morphology and dimension. The turbinate region appeared to experience the most noticeable growth during the first five years of life. The nasal airway volumes of the 10-day, 7-month, 3-year, and 5-year old subjects were 6.4%, 18.8%, 24.2% and 40.3% that of the adult, respectively. Remarkable inter-group variability was observed in airflow, pressure drop, deposition fraction, and particle accumulation. The CFD predicted pressure drops and deposition fractions were in close agreement with *in vitro* measurements.

CONCLUSIONS: Age effects are significant in both breathing resistance and micrometer particle deposition. The image-CFD coupled method provides an efficient and effective approach in understanding patient-specific airflows and particle deposition, which have important implications in pediatric inhalation drug delivery and respiratory disorder diagnosis.

Key words: Nasal physiology; child-adult discrepancy; infants; breathing resistance; aerosol deposition; pediatric drug delivery.

RESPIRATORY CARE Paper in Press. Published on July 02, 2013 as DOI: 10.4187/respcare.02568

Introduction

Considerable structural changes occur in human respiratory tracts during early ages, which lead to vast variations in breathing disorders that are specific to children. Compared to adults, infants and children are more susceptible to respiratory distresses due to their immature defense mechanism. Respiratory disease remains a leading cause of childhood morbidity in the U.S. and other developed countries and is a leading cause of childhood deaths worldwide. Only by understanding the developmental respiratory system can we formulate effective protocols to treat an impaired physiology in pediatric patients.

A number of *in vivo* studies have been conducted to understand the development of respiratory physiology of early ages. Summaries of such studies can be found in recent reviews by Bassham et al.[1] and Ghuman et al.[2] However, these studies mainly focused on the lower respiratory tract. Very few studies have considered the development of upper airway physiology.[3] Clinical techniques for evaluating nasal pathology include visual analog scales [4], rhinostereometry [5], video-endoscopy [6], rhinomanometry [7], and acoustic rhinometry[8]. A combination of the above techniques are usually employed in practice based on the specific performance of each technique[9-12]. Compared with clinical studies, computational fluid dynamics (CFD) predictions have the advantage of providing detailed information on airflow and aerosol deposition, such as regional dosage that are more relevant to health outcome than the average deposition. However, to the authors' knowledge, very few CFD studies have been reported so far studying the nasal physiology of children; one exception is Xi et al. [13] who examined the upper airway structure and associated airflow dynamics in a 5-year-old child. The general neglect of child and infant airways in previous studies may largely be attributed to

RESPIRATORY CARE Paper in Press. Published on July 02, 2013 as DOI: 10.4187/respcare.02568

limited accessibility of pediatric medical images to CFD practitioners, as well as the complexities involved in constructing physiologically realistic nasal passages.

The objective of this study is to characterize the growth of the upper airway in four subjects aged from 10-day to 5-year old using a coupled image-CFD approach. Specific aims are: (1) developing anatomically accurate airway models of children based on CT/MRI images; (2) quantifying the airway dimensions; (3) numerically and experimentally determining the nasal-laryngeal resistance; and (4) numerically determining the inhaled particle deposition. Results of this study may lead to a better understanding of the developmental respiratory physiology and its effects on children's health responses to environmental exposure, or the outcomes from inhalation therapy for infants and children.

Methods

Nasal-Laryngeal Airway Models

One example was used to illustrate the computer method to develop respiratory airway models based on CT/MRI images. Figure 1 shows the procedures of translating the 2-D MRI scans of a health 5-year-old boy (weight 21 kg and height 109 cm)[13] into a 3-D model. The image tracings (Fig. 1a) contained 128 slices that were spaced 1.5 mm apart and spanned from the nostrils to the upper trachea. The multi-slice tracings were segmented in MIMICS (Materialise, Ann Arbor, MI) according to the contrast between soft tissue and intranasal air to isolate the nasal-laryngeal airway, which was further converted into a set of cross-sectional contours that define the airway. Based on these contours, an internal nasal surface geometry was constructed in ANSYS Workbench (Ansys, Inc.). The surface model could be either printed as an *in vitro* cast with 3-D prototyping techniques for experimental purposes (Fig. 1b) or be

RESPIRATORY CARE Paper in Press. Published on July 02, 2013 as DOI: 10.4187/respcare.02568

discretized into a computational mesh for numerical analysis (Fig. 1c). Due to the high complexity of the model geometry, an unstructured tetrahedral mesh was created with high-resolution pentahedral elements in the near-wall region (Fig. 1c). Respiratory geometry retained in this example extended from the nostrils to the upper trachea. In particular, anatomical details such as the epiglottal fold and laryngeal sinuses were retained (Fig. 1a). The resulting model was intended to accurately represent the anatomy of the upper airway with only minor surface smoothing.

Study Design

Age effects on airway physiology, airflow, pressure drop, and inhaled particle deposition were assessed among five subjects aged from 10 days to 53 years old. The CT scans of the three young children (10 days, 7 months, and 3 years old) were provided by Arkansas Children Hospital with no health information disclosed, and their use has been approved by the UAMS Institutional Review Board. Steady inhalations were assumed for all simulations with a wide spectrum of breathing conditions (1–45 L/min). Comparison among the five subjects under equivalent physical activities (quiet breathing) were also conducted based on published respiratory parameters[14-16]. Table 1 shows the literature-based inhalation flow rates under quiet breathing, which were selected to be 3.8 L/min for the 10-day-old girl (10-D-F), 6.5 L/min for the 7-month-old girl (7-M-F), 8.6 L/min for the 3-year-old girl (3-Y-F), 11.2 L/min for the 5-year-old boy (5-Y-M), and 18 L/min for the 53-year-old male adult (53-Y-M). Interestingly, the tidal volumes in the five subjects were observed to intimately correlate with the nasal-laryngeal airway volumes. As shown in Tables 1 and 2, relative to the adult, the tidal volume ratios for 10-D-F, 7-M-F, 3-Y-M, and 5-Y-M were respectively 4.4%, 17.4%, 26.0%, and 35.4%, while the

RESPIRATORY CARE Paper in Press. Published on July 02, 2013 as DOI: 10.4187/respcare.02568

airway volume ratios were respectively 6.4%, 18.8%, 24.0, and 40.3%. Based on the nostril areas in Table 3, the inlet velocities were similar among the five subjects under quiet breathing conditions. Initial particle velocities were assumed to be the same as the local fluid velocity. The airway surface was assumed to be smooth and rigid with a no-slip ($u_{wall} = 0$) condition.

Pressure Measurement

Pressure drops through the *in vitro* casts of the subjects at varying ages were measured using a pressure meter (Magnehelic Gage, Dwyer Instrument Inc., Michigan City, IN). The cast inlets (i.e., nostrils) were open to room air, and a vacuum was connected to the outlet. The pressure meter was positioned immediately after the outlet of the cast to measure the outlet pressure. Pressure drop was obtained for constant inhalation flow rates between 1 and 48 L/min by adjusting the valve on the vacuum line. The flow rate was measured at the outlet using a flow meter (Model 4140, TSI Inc., Shoreview, MN) positioned upstream of the flow valve.

Numerical Method

The low Reynolds number (LRN) k-ω model was selected to simulate the airflow dynamics based on its ability to accurately predict pressure drop, velocity profiles, and shear stress for multi-regime flows.[13, 17-19] It is noted that the LRN k-ω model applies to both laminar and turbulent flow regimes. Deposition fraction was calculated as the ratio of the amount of particles deposited on the airway surface to the amount of particles entering the nostrils. The transport and deposition of inhaled particles are simulated with a well-tested discrete Lagrangian tracking model enhanced with near-wall treatment. The inhaled particles were assumed to be dilute and had no influence upon the continuous-phase, i.e., one-way coupled particle motion. In

RESPIRATORY CARE Paper in Press. Published on July 02, 2013 as DOI: 10.4187/respcare.02568

our previous studies, the Lagrangian tracking model enhanced with user-defined routines was shown to provide a close match to experimental deposition data in upper respiratory airways for both submicrometer [18] and micrometer particles [17].

To establish grid-independent results, convergence sensitivity analysis was conducted following Xi et al. [17]. The final grids for reporting flow field consisted of 1.6–2.0 million cells with a thin five-layer pentahedral grid in the near-wall region and a cell height of 0.05 mm in the first layer (Fig. 1c). The final number of particles tracked was 60,000; increasing the number of tracked particles did not alter the deposition fractions.

Results

Airway Morphological and Dimensional Variations

Significant discrepancies in the nasal-laryngeal airways among the five subjects (10-D-F, 7-M-F, 3-Y-F, 5-Y-M, 53-Y-M) are found in terms of both morphology (Fig. 2) and dimension (Fig. 3). Considering the nasal morphology, younger subjects have smaller sized nostrils, a shorter turbinate region, a more slender nasopharynx, and a thinner pharynx-larynx. Moreover, the nostril shape appears circular at birth, becomes more oval during infancy and childhood, and eventually evolves into a wedge shape in adults[20]. Of particular interest is the turbinate region that seems to be undeveloped in both 10-D-F newborn and 7-M-F infant and is much simpler in morphology compared to those of the children and adult considered in this study. The inferior meatus is missing in the 10-D-F. The inferior and middle meatuses grow with age both in size and complexity, as shown in Fig. 2.

A quantitative comparison of airway dimensions among these five subjects is shown in Fig. 3 in terms of coronal cross-sectional area and perimeter as a function of distance from the

RESPIRATORY CARE Paper in Press. Published on July 02, 2013 as DOI: 10.4187/respcare.02568

nose tip. Comparison of airway volume and surface area in different anatomic sections are listed in Tables 2 and 3. In Table 2, the nasal airway volumes of the 10-D-F, 7-M-F, 3-Y-F, and 5-Y-M are 6.4%, 18.8%, 24.2% and 40.3% that of the 53-Y-M, respectively. The nasal airway surface areas are 22.7%, 30.0%, 41.7% and 65.7% that of the adult, respectively (Table 3). In particular, two major disparities are noted in light of the nasopharynx and nasal valve. First, compared to the adult, children have a much smaller and narrower nasopharynx (NP) lumen. From Fig. 3a, the NP cross-sectional areas of the 10-D-F (A = 31 mm^2), 7-M-F (A = 78 mm^2), 3-Y-F (A = 29 mm^2) and 5-Y-M (A = 170 mm^2) are only 5.8%, 15%, 5.4% and 32% that of the adult (A = 535 mm^2), respectively. The NP hydraulic diameters ($d_h = 4A/Perimeter$) of the 10-D-F (d_h = 5.7 mm), 7-M-F (d_h = 8.1 mm), 3-Y-F (d_h = 4.0 mm), and 5-Y-M (d_h = 12.2 mm) are about 1/4, 1/3, 1/6 and 1/2 that of the adult (i.e., d_h = 24.0 mm), respectively. Specifically, the 3-Y-F seems to have an abnormal NP which is more slender and more constricted than the other three young subjects. The second major disparity is the nostril-valve distances which are much shorter in the two infants (8.0 mm for 10-D-F and 11.2 mm for 7-M-F, Fig. 3a) compared to the two elder children (~20.0 mm) and adult (27.2 mm). The nasal valve cross-sectional areas are likewise smaller for the two youngest subjects (i.e., ~41.7 mm^2 for 10-D-F and ~56 mm^2 for 7-M-F) in compared with the two elder children and adult (Fig. 3a).

Airflow and Breathing Resistance

Nasal airflows under quiet breathing conditions in the five subjects are visualized in Fig. 4a as streamlines within the right nasal passage. Flows of high velocity magnitude are observed in the middle portion of the nasal passage for all models considered. The main flow changes its direction dramatically from the nostrils to the nasopharynx, forming a nearly 180^o curvature.

RESPIRATORY CARE Paper in Press. Published on July 02, 2013 as DOI: 10.4187/respcare.02568

However, this curvature is less severe for the 7-M-F infant model compared to the other three, presumably resulting from a more back-tilted head position of the infant during image acquisition. The airflow speed is higher in the NP of the 3-Y-F due to the severe NP constriction. No recirculation zone is observed in the NP of the three young subjects due to a much smaller airway diameter in this region, which differs from the adult NP where flow recirculation is obvious (Fig. 4a).

Airflow dynamics within the nasal passages are further visualized in Fig. 4b as snapshots of particle locations at selected instants. Two thousand 1.0 μm particles were released at the right nostril at t = 0 second and particle positions were recorded after designated periods of time. Due to the small inertia, 1.0 μm particles are assumed to closely follow the airflow. Faster transport and deeper penetration of aerosols are apparent in the medial passages, while slow-moving particles are found near the airway walls. Because of the dramatic airway bend from the nostrils to the nasopharynx, a high-concentration of particles constantly adjust their directions following the mean streamline curvature of inhaled airflows. The seemingly random particle distributions in the pharynx indicate enhanced turbulent mixing in this region. Due to the smaller nasopharynx-larynx regions in children, particles are transported faster and reach the glottal aperture faster than in the adult. This difference is more pronounced in the 3-Y-F who possesses an abnormally slender naso- and velo-pharynx.

The comparison of measured and CFD-predicted pressure drop (Δp) among the five subjects is shown in Fig. 5 for a wide spectrum of breathing conditions (1–48 L/min). All subjects considered are in close agreements. It is noted that the *in vitro* experiments and CFD-predictions have been conducted in the same airway geometry models so that a direct comparison is possible. In general, the pressure drop (i.e., breathing resistance) decreases as the

RESPIRATORY CARE Paper in Press. Published on July 02, 2013 as DOI: 10.4187/respcare.02568

age increases (Fig. 5a). For a given flow rate, infants and children have much higher breathing resistances than the adult. However, it is also not surprising to observe that the 3-Y-F model gives a much higher pressure drop than the 7-M-F, considering the abnormally constricted nasopharynx in the 3-Y-F as well as the less severe airway curvature in the 7-M-F. The flow-pressure relationships can be expressed as a power function ($\Delta P = a \cdot Q^b$), which can be plotted as straight lines on a log-log scale with a slope of "*b*", as shown in Fig. 5b. The best-fitted coefficients "*a*" and "*b*" for subjects of different ages are listed in Table 4.

Particle Deposition

Particle deposition in the nasal-laryngeal airway of the 5-year-old boy is displayed in Fig. 6a for particles ranging from 2.5–40 μm at a flow rate of 10 L/min. Highly heterogeneous particle distributions are noted for all particle sizes considered. Moreover, the variation of deposition location with particle size is clearly shown in this example. Particles of 40 μm or larger are mostly filtered out at the nasal vestibule region (gray points in Fig. 6a) and cannot be inhaled. For those respirable aerosols, larger particles (20 μm) are found to deposit mainly in the superior and middle nasal passages due to their higher inertia. The deposition of smaller particles (10 μm) shifts downward and is mainly observed in the middle passage. The even smaller particles (2.5 μm), which can closely follow the mainstream airflow, are observed mainly in the middle and inferior passages.

The deposition fraction as a function of particle aerodynamic diameter is shown in Fig. 6b in comparison with existing experimental data. The inhalation flow rates considered are 10 and 20 L/min and the particle sizes range from 0.5–32 μm. The *in vitro* experiments of Zhou et al. [21] and the current CFD predictions are based on the same airway geometry model. Again,

RESPIRATORY CARE Paper in Press. Published on July 02, 2013 as DOI: 10.4187/respcare.02568

close matches are observed between the predicted and the measured deposition data, with slight underestimation by CFD compared to measurements at the flow rate of 20 L/min. For both flow rates considered, particles larger than 10 μm are mostly filtered out in this pediatric nasal-laryngeal airway (i.e., the cut size being 10 μm). For particles smaller than 10 μm, the deposition rate exhibits a high sensitivity to the aerosol size and flow rate, which increases quickly as the aerosol size or flow rate increases.

The age-related effects on nasal depositions among the five subjects are shown in Fig. 7 under equivalent physical activity (i.e., sedentary) conditions. The particle sizes considered are 2.5 μm and 10 μm. Large variability is observed among the five models, both in deposition pattern (Fig. 7a) and regional deposition fractions (Fig. 7b). For small particles (2.5 μm), deposition fractions are very low in the three regions of each model (i.e., anterior, middle, and posterior). One exception is the 3-year-old girl model, whose elevated deposition is presumably attributed to the more constricted nasopharynx. For large particles (10 μm), nasal depositions increase by approximately one order of magnitude. Again, the highest deposition is found in the 3-year-old model. Considering regional depositions, the allocation of deposition fractions in the three regions differs for 2.5 and 10 μm particles in each model considered. For 2.5 μm particles, the anterior region (nasal vestibule and valve) generally receives more particles than the others. In contrast, the middle (turbinate) region receives more deposition for 10 μm particles (Fig. 7b). A high deposition of 10 μm particles is found in the anterior region in the adult model, but not in the infant and child models. If considering the anterior and middle regions together (nasal passage), the adult model filters more 10 μm particles than the children. This may result from the higher complexity of the adult nasal passages.

RESPIRATORY CARE Paper in Press. Published on July 02, 2013 as DOI: 10.4187/respcare.02568

Discussion

There is enormous physiological growth during infancy and childhood. Significant differences were noted in the nose-throat anatomy among the five subjects of different ages. These differences manifest themselves not only in airway dimension but also in airway morphology. For example, the nasal-laryngeal airway volumes of the 10-D-F, 7-M-F, 3-Y-F, and 5-Y-M are 6.4%, 18.8%, 24.2%, and 40.3% that of the 53-Y-M, respectively. At the same time, the four young subjects have smaller sized nostrils, a shorter turbinate region, and a more slender nasopharynx. Results of this study indicate that the nasal valve and vestibule region might mature between the ages three and five. This is supported by the much shorter nostril-valve distance and much smaller cross-sectional area of the nasal valve in the two infants compared to the two elder children as well as the proximity of the these two parameters between the adult and two elder children (Fig. 3a). Specifically, the nostril-valve distances are 8.0–11.2 mm for the two infants *vs.* 19.0–20.8 mm for the two children and 27.2 mm for the adult; the nasal valve areas are 42–56 mm^2 for the infants *vs.* 120–180 mm^2 for the children and adult. Another observation is that the turbinate region experiences fast growth from birth to the age of five, as indicated by the remarkable volume increase of this region (i.e., 1.57 cm^3 for 10-D-F, 2.83 cm^3 for 7-M-F, 5.83 for 3-Y-F, 11.03 cm^3 for 5-Y-M, and 12.63 cm^3 for 53-Y-M in Table 2). However, a lack of similarity in shape between the 5-Y-M and adult may still indicate an undeveloped turbinate region at the age of five. It is apparent that the nasopharynx grows the least compared to other respiratory anatomies during the first five years of life (i.e., volume = 0.48 cm^3 for 10-D-F, 1.74 cm^3 for 7-M-F, 1.07 cm^3 for 3-Y-F, 3.95 cm^3 for 5-Y-M, and 16.33 cm^3 for 53-Y-M, Table 2). Further studies on more age groups are necessary to quantify the

RESPIRATORY CARE Paper in Press. Published on July 02, 2013 as DOI: 10.4187/respcare.02568

developmental respiratory physiology and their associated effects on breathing and aerosol filtration.

A power function ($\Delta P = a \cdot Q^b$) has been used to correlate the respiratory rate and airway pressure drop in previous inhalation studies.[22, 23] The flow-pressure relation shows high sensitivity to age in this study, as indicated by the large variation of "*b*" for different age groups (8.73–0.16 from 10-D-F to 53-Y-M, Table 4). It is noted that for an equivalent physical activity, the inhalation rates are different for different age groups due to their particular respiratory variables such as frequency, I:E ratio, and tidal volume. Based on the selected flow rates (i.e., 3.8 L/min for 10-D-F, 6.5 L/min for 7-M-F, 9.5 L/min for 3-Y-F, 11.2 L/min for 5-Y-M, and 18 L/min for 53-Y-M), the nasal breathing resistance is maximum for 10-D-F, and decreases as age increases for normal subjects. Furthermore, this decrease appears most dramatic in the first year (10-D-F to 7-M-F herein), and the rate of decrease become gradually smaller beyond this age. Interestingly, a similar observation in respiratory rates was reported by Fleming et al.[15] who studied 3381 children and showed a constant decline in respiratory rate from birth to adolescence, with the steepest fall in infants under 2 years of age.

The flow-pressure relation also shows high sensitivity to airway abnormalities, as suggested by the abrupt increase in magnitude of "*b*" for the 3-Y-F who has a more constricted nasopharynx (Table 4). In this case, the subject may expect increased respiratory efforts when awake and obstructive sleep apnea symptoms during sleep. Results of this study indicate that computational modeling could be a supplemental tool to study breathing-related disorders. By providing detailed airflow information that is not readily measured by conventional diagnosis techniques [24], additional clues could be unveiled that are clinically relevant to breathing disorders such as snoring and sleep apnea.

RESPIRATORY CARE Paper in Press. Published on July 02, 2013 as DOI: 10.4187/respcare.02568

Deposition patterns of inhaled aerosols are not uniform in human upper airways, with heterogeneous deposition allocations in different anatomic regions. [17, 25, 26] In this study, the regional deposition allocations are observed to vary substantially among different age groups. Considering that tissues receiving higher depositions of toxicants are more vulnerable for injury, such results might help to elucidate the diverse etiology and symptoms of respiratory disorder in different subjects or age groups. The deposition partition in the three regions considered (i.e., vestibule-valve, turbinate, and nasopharynx) is remarkably different among the five subjects, indicating a different level of risks upon the region of interest even when exposed to the same environment. The higher turbinate deposition in the 3-year-old may suggest a higher chance of nasal inflammation and exacerbate existing symptoms of difficult breathing. On the other hand, outcomes from inhalation therapies require drugs to be delivered to the targeted tissues at a sufficient dose. The heterogeneity in regional depositions among subjects of different ages implies that existing adult deposition results might not guarantee an accurate dosimetry planning for infants and children.

Limititions

Limitations of this study include the assumptions of steady flows, quiet breathing only, rigid airway walls, idealized particles, and a limited number of samples per age group. Other studies have highlighted the physical significance of tidal breathing[27], effects of physical activities[27], airway wall motion[28], and nasal valve collapse[29]. Besides, environmental aerosols are mostly non-spherical[30], interacting among themselves[31], and may undergo changes in size due to hygroscopic effect[32] or coagulation[33]. Moreover, each model in this study is based on images of one single subject and does not account for the intersubject variability which can be

RESPIRATORY CARE Paper in Press. Published on July 02, 2013 as DOI: 10.4187/respcare.02568

significant[34, 35]. Another limitation is the typical supine position of the subjects during data acquisition, which is different from sedentary breathing. Images acquired at the end of the inhalation may not reflect variations in airway geometry during a full breathing cycle. Therefore, future studies are needed that should be orientated toward: (1) improving physical realism and (2) including a broader population group. Our knowledge of nasal deposition is currently lacking in subpopulations such as pediatrics, geriatrics, and patients with respiratory diseases. Due to physiological development, aging, or disease states, the airway anatomy can be remarkably different from that of a healthy adult. Concentrating on these specific subpopulations will help to clarify inter-group and inter-individual variability and will allow for the design of more efficient pharmaceutical formulations and drug delivery protocols for different age groups. In addition, further methodology developments and deposition measurements are required to provide robust estimates of airway depositions of either airborne contaminants or inhaled pharmacological particles.

Conclusions

Significant variability exists in airway physiology, airflow dynamics, and aerosol deposition among subjects of different ages. Specific observations include:

(1) The nasal airway volumes of the 10-D-F, 7-M-F, 3-Y-F, and 5-Y-M are 6.4%, 18.8%, 24.2% and 40.3% that of the 53-Y-M adult, respectively; while the nasal airway surface areas are 22.7%, 30.0%, 41.7%, and 65.7% that of the adult, respectively.

(2) The airway pressure drop is sensitive to a person's age and airway abnormalities. Flow-pressure correlations have been proposed for different age groups based on a wide range of breathing conditions.

RESPIRATORY CARE Paper in Press. Published on July 02, 2013 as DOI: 10.4187/respcare.02568

(3) Age effects are large in both total and regional deposition rates and should be considered in future environmental health assessment and inhalation drug delivery.

(4) Satisfactory agreements between CFD-predictions and *in vitro* experiments were obtained in pressure drop and particle deposition, indicating that the image-CFD coupled method is a practical tool in diagnosing respiratory disorders and developing effective inhalation devices.

RESPIRATORY CARE Paper in Press. Published on July 02, 2013 as DOI: 10.4187/respcare.02568

References

1. Bassham BS, Kane I, MacKeil-White K, Fischer J, Arnold D, Whatley V, et al. Difficult airways, difficult physiology and difficult technology: respiratory treatment of the special needs child. Clinical Pediatric Emergency Medicine 2012;13(2):81-90.
2. Ghuman AK, Newth CJL, Khemani RG. Respiratory support in children. Paediatrics and Child Health 2011;21(4):163-169.
3. Brodsky L. Chapter 35 - Structure and Development of the Upper Respiratory System in Infants and Children. Pediatric Critical Care (Fourth Edition). Saint Louis: Mosby, 2011:485-489.
4. Ernstgard L, Bottai M. Visual analogue scales: how can we interpret them in experimental studies of irritation in the eyes, nose, throat and airways? Journal of Applied Toxicology 2012;32(10):777-782.
5. Ellegard E. Practical aspects on rhinostereometry. Rhinology 2002;40(3):115-117.
6. Keck T, Leiacker R, Kuhnemann S, Lindemann J, Rozsasi A, Wantia N. Video-endoscopy and digital image analysis of the nasal valve area. European Archives of Oto-Rhino-Laryngology 2006;263(7):675-679.
7. Demirbas D, Cingi C, Cakli H, Kaya E. Use of rhinomanometry in common rhinologic disorders. Expert Review of Medical Devices 2011;8(6):769-777.
8. Wheeler SM, Corey JP. Evaluation of upper airway obstruction - an ENT perspective. Pulmonary Pharmacology & Therapeutics 2008;21(3):433-441.
9. Kesavanathan J, Swift DL, Fitzgerald TK, Permutt T, Bascom R. Evaluation of acoustic rhinometry and posterior rhinomanometry as tools for inhalation challenge studies. Journal of Toxicology and Environmental Health 1996;48(3):295-307.

RESPIRATORY CARE Paper in Press. Published on July 02, 2013 as DOI: 10.4187/respcare.02568

10. Pirila T, Nuutinen J. Acoustic rhinometry, rhinomanometry and the amount of nasal secretion in the clinical monitoring of the nasal provocation test. Clinical and Experimental Allergy 1998;28(4):468-477.

11. Porter MJ, Williamson IG, Kerridge DH, Maw AR. A comparison of the sensitivity of manometric rhinometry, acoustic rhinometry, rhinomanometry and nasal peak flow to detect the decongestant effect of xylometazoline. Clinical Otolaryngology 1996;21(3):218-221.

12. Pirila T, Tikanto J. Acoustic rhinometry and rhinomanometry in the preoperative screening of septal surgery patients. American Journal of Rhinology & Allergy 2009;23(6):605-609.

13. Xi J, Si X, Kim JW, Berlinski A. Simulation of airflow and aerosol deposition in the nasal cavity of a 5-year-old child. Journal of Aerosol Science 2011;42(3):156-173.

14. Gagliardi L, Rusconi F, Castagneto M, Porta GLN, Razon S, Pellegatta A. Respiratory rate and body mass in the first three years of life. Archives of Disease in Childhood 1997;76(2):151-154.

15. Fleming S, Thompson M, Stevens R, Heneghan C, Plüddemann A, Maconochie I, et al. Normal ranges of heart rate and respiratory rate in children from birth to 18 years of age: a systematic review of observational studies. The Lancet 2011;377(9770):1011-1018.

16. Rusconi F, Castagneto M, Porta N, Gagliardi L, Leo G, Pellegatta A, et al. Reference values for respiratory rate in the first 3 years of life. Pediatrics 1994;94(3):350-355.

17. Xi J, Longest PW. Transport and deposition of micro-aerosols in realistic and simplified models of the oral airway. Annals of Biomedical Engineering 2007;35(4):560-581.

18. Xi J, Longest PW. Effects of oral airway geometry characteristics on the diffusional deposition of inhaled nanoparticles. ASME Journal of Biomechanical Engineering 2008;130:011008.

19. Xi J, Longest PW, Martonen TB. Effects of the laryngeal jet on nano- and microparticle transport and deposition in an approximate model of the upper tracheobronchial airways. Journal of Applied Physiology 2008;104:1761-1777.

20. Xi J, Longest PW. Numerical predictions of submicrometer aerosol deposition in the nasal cavity using a novel drift flux approach. International Journal of Heat and Mass Transfer 2008;51(23-24):5562-5577.

21. Zhou Y, Xi J, Simpson J, Irshad H, Cheng YS. Aerosol deposition in a nasopharyngolaryngeal replica of a 5-year-old child. Aerosol Science and Technology 2013;47:275-282.

22. Garlick SR, Gehring JM, Wheatley JR, Amis TC. Nasal airflow resistance and the flow resistive work of nasal breathing during exercise: Effects of a nasal dilator strip. American Journal of Respiratory and Critical Care Medicine 1999;159(3):A417-A417.

23. Wheatley JR, Amis TC, Engel LA. Nasal and oral airway pressure-flow relationships. Journal of Applied Physiology 1991;71(6):2317-2324.

24. Flemons WW, Buysse D, Redline S, Pack A, Strohl K, Wheatley J, et al. Sleep-related breathing disorders in adults: Recommendations for syndrome definition and measurement techniques in clinical research. Sleep 1999;22(5):667-689.

25. Si X, Xi J, Kim JW, Zhou Y, Zhong H. Modeling of release position and ventilation effects on olfactory aerosol drug delivery. Respiratory Physiology and Neurobiology 2013;186:22-32.

26. Xi J, Longest PW. Evaluation of a drift flux model for simulating submicrometer aerosol dynamics in human upper tracheobronchial airways. Annals of Biomedical Engineering 2008;36(10):1714-1734.

27. Haussermann S, Bailey AG, Bailey MR, Etherington G, Youngman M. The influence of breathing patterns on particle deposition in a nasal replicate cast. Journal of Aerosol Science 2002;33(6):923-933.

28. Fodil R, Brugel-Ribere L, Croce C, Sbirlea-Apiou G, Larger C, Papon JF, et al. Inspiratory flow in the nose: a model coupling flow and vasoerectile tissue distensibility. Journal of Applied Physiology 2005;98(1):288-295.

29. Bridger GP, Proctor DF. Maximum nasal inspiratory flow and nasal resistance. Annals of Otology, Rhinology & Laryngology 1970;79(3):481-488.

30. Tian L, Ahmadi G, Wang ZC, Hopke PK. Transport and deposition of ellipsoidal fibers in low Reynolds number flows. Journal of Aerosol Science 2012;45:1-18.

31. Nasr H, Ahmadi G, McLaughlin JB. A DNS study of effects of particle-particle collisions and two-way coupling on particle deposition and phasic fluctuations. Journal of Fluid Mechanics 2009;640:507-536.

32. Longest PW, Xi JX. Condensational growth may contribute to the enhanced deposition of cigarette smoke particles in the upper respiratory tract. Aerosol Science and Technology 2008;42(8):579-602.

33. Okuyama K, Kousaka Y, Hayashi K. Change in size distribution of ultrafine aerosol particles undergoing Brownian coagulation. Journal of Colloid and Interface Science 1984;101(1):98-109.

RESPIRATORY CARE Paper in Press. Published on July 02, 2013 as DOI: 10.4187/respcare.02568

34. Storey-Bishoff J, Noga M, Finlay WH. Deposition of micrometer-sized aerosol particles in infant nasal airway replicas. Journal of Aerosol Science 2008;39(12):1055-1065.

35. Garcia GJM, Tewksbury EW, Wong BA, Kimbell JS. Interindividual variability in nasal filtration as a function of nasal cavity geometry. Journal of Aerosol Medicine and Pulmonary Drug Delivery 2009;22(2):139-155.

RESPIRATORY CARE Paper in Press. Published on July 02, 2013 as DOI: 10.4187/respcare.02568

Figure Legends

Fig. 1. Nasal-laryngeal airway model development: (a) 3D rendering of medical images of a 5-year-old boy for (b) *in vitro* measurement and (c) numerical analysis. The nasal airway was divided into different anatomical sections: nasal vestibule and valve region (V&V), nasal turbinate (TR), nanopharynx (NP), pharynx, and larynx. The computational mesh is composed of approximately 1.8 million unstructured tetrahedral elements and fine near-wall pentahedral grid.

Fig. 2. Image-based nasal-laryngeal airway models of a 10-day-old girl, a 7-month-old girl, a 3-year-old girl, and a 5-year-old boy in comparison with a 53-year-old male.

Fig. 3. Comparison of the nasal dimensions among subjects of different ages as a function of the distance from the nose tip: (a) cross-sectional area and (b) perimeter. The nasal valve (i.e., minimum cross-sectional area) in each model is marked by an arrow in panel (a).

Fig. 4. Inhalation airflow inside the nasal-laryngeal airways under quiet breathing conditions: (a) streamlines (right passage); and (b) flow pattern visualized with mass-less fluid particles at various instants.

Fig. 5. Comparison of measured and computed pressure drops in the nasal-laryngeal airways of different ages: (a) linear diagram, and (b) logarithm diagram.

Fig. 6. Particle deposition in the nasal-laryngeal airway of the 5-year-old boy. (a) heterogeneous deposition distributions were observed on the airway surface, and (b) close matches were obtained between the measured and computed deposition fractions for both 10 L/min and 20 L/min.

RESPIRATORY CARE Paper in Press. Published on July 02, 2013 as DOI: 10.4187/respcare.02568

Fig. 7. Comparison of (a) surface deposition and (b) sub-regional deposition fractions among the five models under quiet breathing conditions. Model surfaces are 50% translucent.

RESPIRATORY CARE Paper in Press. Published on July 02, 2013 as DOI: 10.4187/respcare.02568

Tables:

Table 1. Respiratory parameters under quiet breathing conditions at various ages based on references[14-16]

Respir. Variable	10-D-F	7-M-F	3-Y-F	5-Y-M	53-Y-M
Frequency (/min)	44	25	22	21	12
I:E* ratio	1:3	1:2	1:2	1:2	1:2
Inhalation (s)	0.34	0.8	0.9	0.95	1.67
Tidal vol (mL)	22	87	130	177	500
TV Ratio‡ (%)	4.4	17.4	26.0	35.4	100
Flow rate (L/min)	3.8	6.5	8.6	11.2	18.0
Inlet vel (m/s)	1.91	1.84	1.66	1.84	1.48

10-D-F: 10-day-old female, 5-Y-M: 5-year-old male
*I:E ratio: Inspiratory to Expiratory ratio.
‡ TV Ratio: the ratio of tidal volume to that of the adult.

Table 2. Airway volume

Vol (cm^3)	10-D-F	7-M-F	3-Y-F	5-Y-M	53-Y-M
V&V*	0.79	1.25	1.41	3.37	5.50
TR*	1.57	2.83	5.83	11.03	12.63
NP*	0.48	1.74	1.07	3.95	16.33
Pharynx	0.31	3.19	3.10	2.64	13.89
Larynx	0.36	1.32	1.92	1.22	6.70
Total:	3.51	10.33	13.32	22.21	55.05
Ratio+(%)	6.4	18.8	24.2	40.3	100

* V&V (vestibule and valve), TR (turbinate region), NP (nasopharynx)
+ Ratio: the ratio of anatomical parameter to that of the adult.

Table 3. Airway surface area

A (cm^2)	10-D-F	7-M-F	3-Y-F	5-Y-M	53-Y-M
V&V	7.45	9.75	18.97	23.74	35.58
TR	21.09	35.63	54.71	107.34	112.59
NP	3.72	9.27	9.79	15.27	40.93
Pharynx	2.96	13.71	13.92	14.59	45.10
Larynx	2.87	8.37	9.46	7.20	12.81
Total:	38.09	76.73	106.85	168.14	256.01
Ratio (%)	22.7	30.0	41.7	65.7	100
Inlets:					
R nostril	0.166	0.280	0.434	0.492	1.013
L nostril	0.166	0.315	0.431	0.437	1.013
Total:	0.332	0.595	0.865	0.929	2.026
Ratio (%)	16.4	29.4	42.7	45.9	100
Outlets:					
Trachea	0.178	0.506	0.671	0.832	1.487
Ratio (%)	12.0	34.0	45.1	56.0	100

RESPIRATORY CARE Paper in Press. Published on July 02, 2013 as DOI: 10.4187/respcare.02568

Table 4. Flow-pressure correlation coefficients

Subject	Image	*a*	*b*
10-D-F	CT	5.86	1.89
7-M-F	CT	1.77	*1.48*
3-Y-F	CT	2.71	*1.84*
5-Y-M	MRI	0.58	1.70
53-Y-M	MRI	0.21	1.71

RESPIRATORY CARE Paper in Press. Published on July 02, 2013 as DOI: 10.4187/respcare.02568

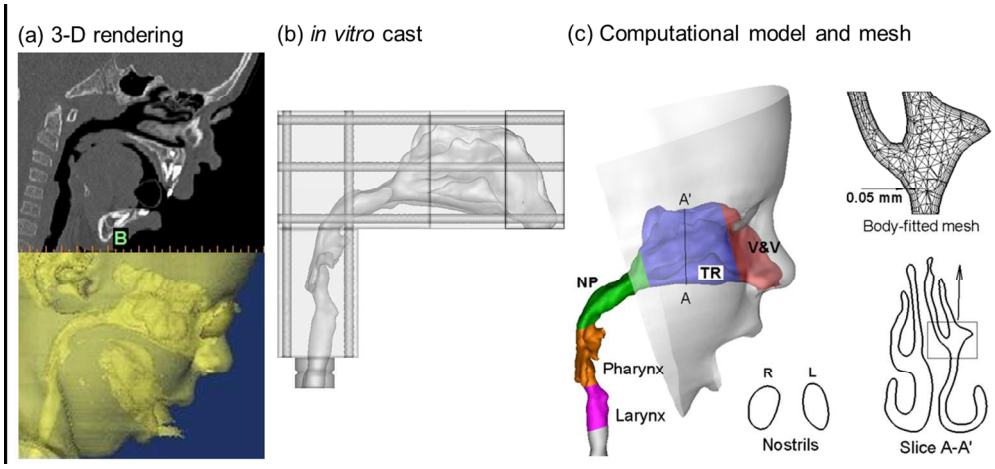

Fig. 1. Nasal-laryngeal airway model development: (a) 3D rendering of medical images of a 5-year-old boy for (b) in vitro measurement and (c) numerical analysis. The nasal airway was divided into different anatomical sections: nasal vestibule and valve region (V&V), nasal turbinate (TR), nanopharynx (NP), pharynx, and larynx. The computational mesh is composed of approximately 1.8 million unstructured tetrahedral elements and fine near-wall pentahedral grid.
254x116mm (150 x 150 DPI)

RESPIRATORY CARE Paper in Press. Published on July 02, 2013 as DOI: 10.4187/respcare.02568

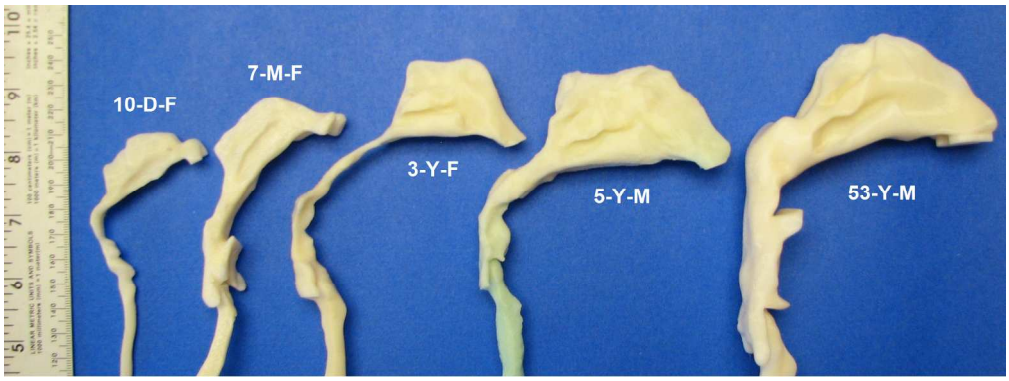

Fig. 2. Image-based nasal-laryngeal airway models of a 10-day-old girl, a 7-month-old girl, a 3-year-old girl, and a 5-year-old boy in comparison with a 53-year-old male.
617x228mm (96 x 96 DPI)

RESPIRATORY CARE Paper in Press. Published on July 02, 2013 as DOI: 10.4187/respcare.02568

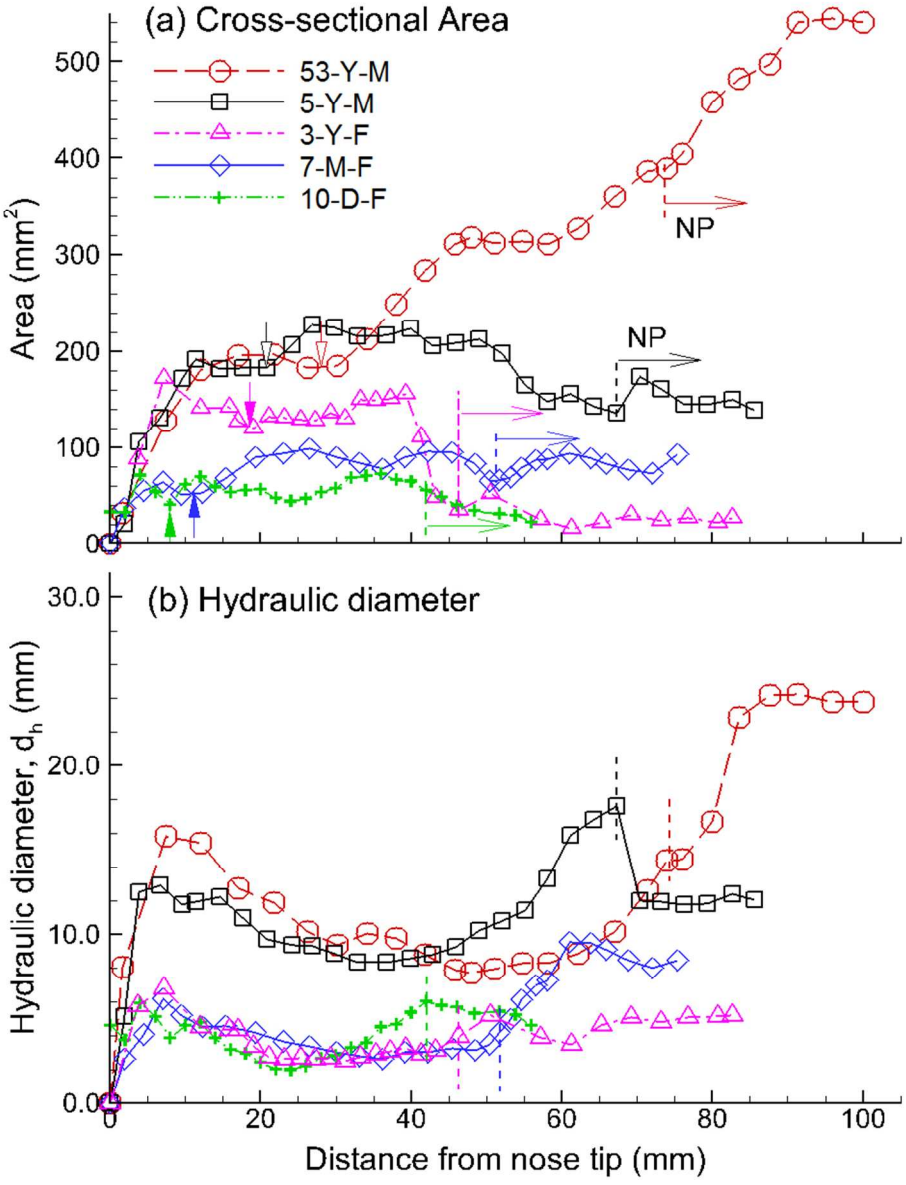

Fig. 3. Comparison of the nasal dimensions among subjects of different ages as a function of the distance from the nose tip: (a) cross-sectional area and (b) perimeter. The nasal valve (i.e., minimum cross-sectional area) in each model is marked by an arrow in panel (a).
264x329mm (96 x 96 DPI)

RESPIRATORY CARE Paper in Press. Published on July 02, 2013 as DOI: 10.4187/respcare.02568

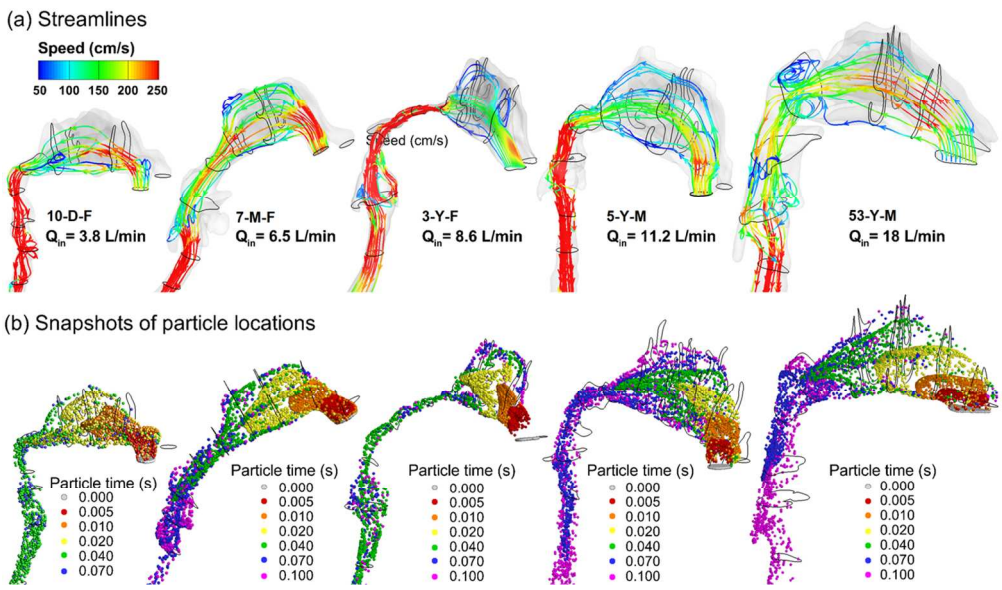

Fig. 4. Inhalation airflow inside the nasal-laryngeal airways under quiet breathing conditions: (a) streamlines (right passage); and (b) flow pattern visualized with mass-less fluid particles at various instants.
249x144mm (150 x 150 DPI)

RESPIRATORY CARE Paper in Press. Published on July 02, 2013 as DOI: 10.4187/respcare.02568

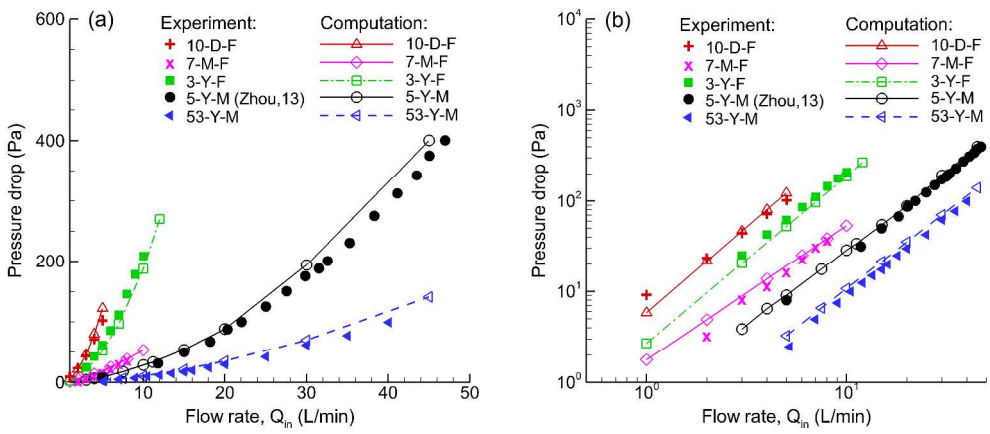

Fig. 5. Comparison of measured and computed pressure drops in the nasal-laryngeal airways of different ages: (a) linear diagram, and (b) logarithm diagram.
793x344mm (96 x 96 DPI)